Performance verification testing for HET wide-field upgrade tracker in the laboratory

Good, John, Hayes, Richard, Beno, Joseph, Booth, John, Cornell, Mark, et al.

John Good, Richard Hayes, Joseph Beno, John Booth, Mark E. Cornell, Gary J. Hill, Hanshin Lee, Jason Mock, Marc Rafal, Richard Savage, Ian Soukup, "Performance verification testing for HET wide-field upgrade tracker in the laboratory," Proc. SPIE 7739, Modern Technologies in Space- and Ground-based Telescopes and Instrumentation, 77393C (23 July 2010); doi: 10.1117/12.857890

SPIE.

Event: SPIE Astronomical Telescopes + Instrumentation, 2010, San Diego, California, United States

Performance Verification Testing for HET Wide-field Upgrade Tracker in the Laboratory

John Good[a†], Richard Hayes[b], Joseph Beno[b], John Booth[a], Mark E. Cornell[a], Gary J.Hill[a], Hanshin Lee[a], Jason Mock[b], Marc Rafal[a], Richard Savage[a], Ian Soukup[b]

[a]McDonald Observatory, University of Texas at Austin, 1 University Station C1402, Austin, TX, USA 78712-0259;
[b]Center for Electro-mechanics, The University of Texas, 1 University Station R7000, Austin, TX, USA 78712

ABSTRACT

To enable the Hobby-Eberly Telescope Dark Energy Experiment (HETDEX), the McDonald Observatory (MDO) and the Center for Electro-mechanics (CEM) at the University of Texas at Austin are developing a new HET tracker in support of the Wide-Field Upgrade (WFU) and the Visible Integral-Field Replicable Unit Spectrograph (VIRUS). The precision tracker is required to maintain the position of a 3,100 kg payload within ten microns of its desired position relative to the telescope's primary mirror. The hardware system to accomplish this has ten precision controlled actuators. Prior to installation on the telescope, full performance verification is required of the completed tracker in CEM's lab, without a primary mirror or the telescope's final instrument package. This requires the development of a laboratory test stand capable of supporting the completed tracker over its full range of motion, as well as means of measurement and methodology that can verify the accuracy of the tracker motion over full travel (4m diameter circle, 400 mm deep, with 9 degrees of tip and tilt) at a cost and schedule in keeping with the HET WFU requirements. Several techniques have been evaluated to complete this series of tests including: photogrammetry, laser tracker, autocollimator, and a distance measuring interferometer, with the laser tracker ultimately being identified as the most viable method. The design of the proposed system and its implementation in the lab is presented along with the test processes, predicted accuracy, and the basis for using the chosen method[*].

Keywords: Hobby-Eberly Telescope, HET, HETDEX, Wide Field Corrector, Tracker, VIRUS, laser tracker, photogrammetry

1. INTRODUCTION

The Hobby-Eberly Telescope (HET) was originally envisioned as a spectroscopic survey telescope, able to efficiently survey objects over wide areas of the sky. While the telescope has been very successful observing large samples of objects such as quasi-stellar objects (QSOs) spread over the sky with surface densities of around one per 10 sq. degrees, the HET design, coupled with a small field of view corrector, hampers programs where objects have higher sky densities. In seeking a strong niche for the HET going forward, the HET field of view will be increased from 4′ to 22′ so that it can accommodate the Visible Integral-field Replicable Unit Spectrograph (VIRUS)[1-5], an innovative, highly multiplexed spectrograph that will open up the emission-line universe to systematic surveys for the first time, uncovering populations of objects selected by their line emission rather than by their continuum emission properties.

The HET will undergo this major upgrade in 2011 to support HETDEX as well as current and future instrumentation. This upgrade project consists of three primary elements:

- HET wide field upgrade (WFU)[6,7] which includes designing, fabricating, and deploying a larger field of view corrector (referred to as the wide field corrector [WFC]) that will replace the existing spherical aberration corrector. It

[*] The Hobby-Eberly Telescope is operated by McDonald Observatory on behalf of the University of Texas at Austin, the Pennsylvania State University, Stanford University, Ludwig-Maximillians-Universität München,and Georg-August-Universität, Göttingen

[†] R.S.: E-mail: good@astro.as.utexas.edu

[‡] http://hetdex.org/

Modern Technologies in Space- and Ground-based Telescopes and Instrumentation, edited by Eli Atad-Ettedgui, Dietrich Lemke, Proc. of SPIE Vol. 7739, 77393C · © 2010 SPIE · CCC code: 0277-786X/10/$18 · doi: 10.1117/12.857890

also requires the design, fabrication, and deployment of a new prime focus instrument package (PFIP) and tracker[8-14], as well as modification to the HET's azimuth bearings, to accommodate the additional weight being added to the telescope.

- Design, fabrication and deployment of VIRUS on HET.
- Execution of the Dark Energy Experiment (DEX) survey with the VIRUS on HET.

Engineering, design, and fabrication of the new tracker is being performed, or managed by CEM, who has a team of 40 multi-disciplinary engineers, 5 technicians, and 6 machinists. This research and development facility is comprised of 8,000 square meters of office space, 10,000 square meters of laboratory and machining facilities with a 21 meter high ceiling, and 22 metric ton bridge crane system. The combined engineering, machining, and laboratory resource is stationed in Austin, Texas and convenient to the main MDO offices allowing convenient development and testing of the tracker prior to shipment and installation at the Observatory.

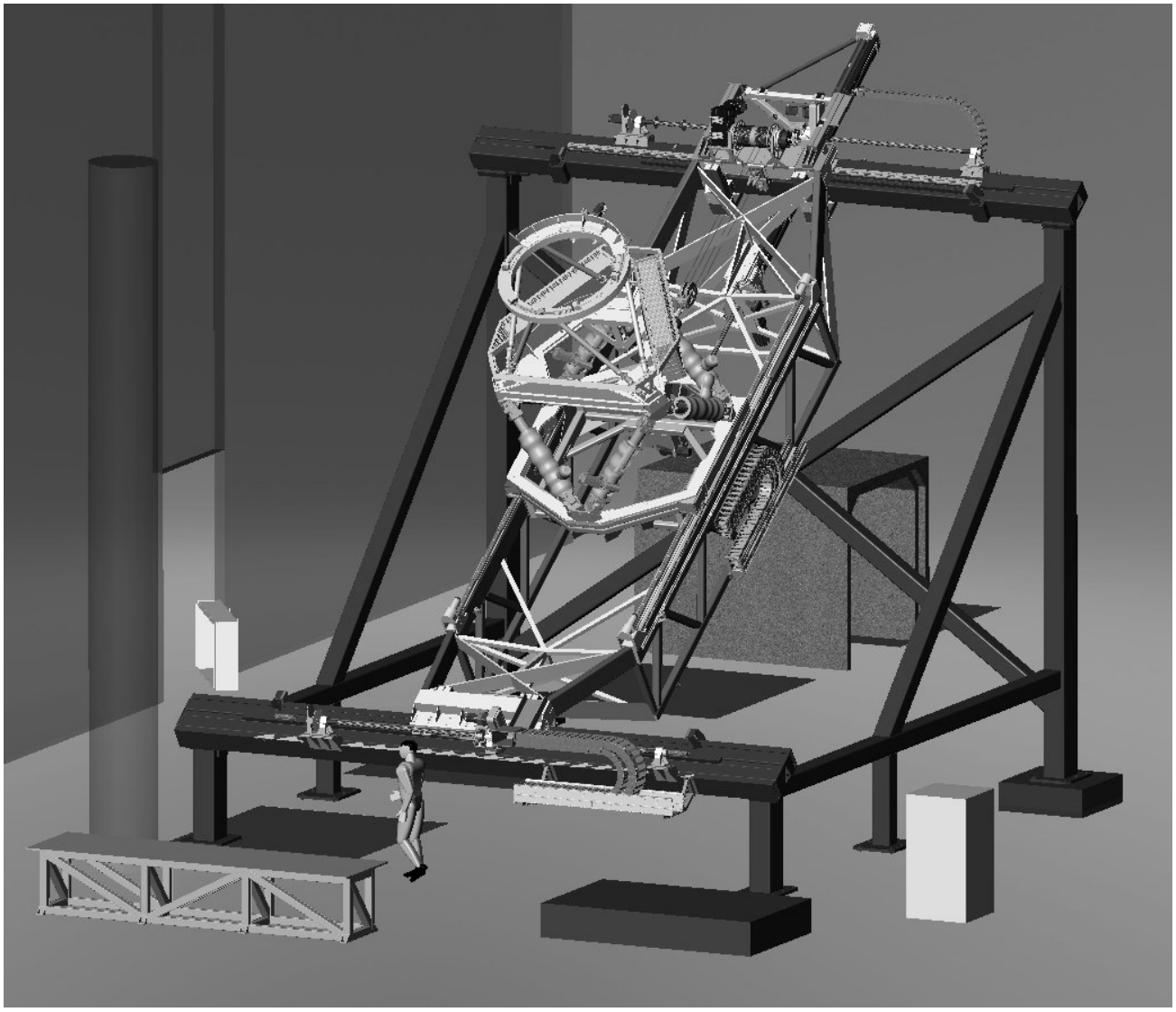

Figure 1. Tracker test stand that will be used to troubleshoot and pre-commission the tracker at CEM prior to installation on the HET.

In order to minimize telescope down-time due to retro-fit and commissioning of the WFU and VIRUS, a plan has been established to set up the tracker on a test stand in the CEM laboratory high-bay for testing. Aside from the need to

precisely align the tracker assembly for proper functioning, it will be important to perform measurements that allow a preliminary mount model to be written and then to independently test the control algorithms for the whole system of 10 axes in order to verify that the tracker is capable of tracking stars *prior* to installation on the HET. Since there is no cost effective way to perform an optical verification of this performance, a process is proposed, combining the metrology capabilities of laser trackers, and data fitting software, that will verify the equivalent motions.

2. LABORATORY CONFIGURATION

The upper portion of the telescope structure is simulated by a test stand configured as shown in Figure 1, in the CEM High-Bay. Additional floor space in the facility will be used for pre-assembly and testing of the tracker bridge assembly, hexapod, and PFIP prior to mounting on the test stand. The upper and lower beams of the tracker test stand are a welded assembly of standard structural Hollow Structural Section (HSS) shapes that duplicate those on the as-built telescope structure, and hold the tracker at an angle of 35 degrees from zenith. Due to the 5x increase in mass of the new tracker the lower beam will be reinforced, ultimately necessitating extensive in-situ welds on the HET structure. Identical reinforcements will be welded on to the lower beam of the test stand in order to establish and refine the weld procedure and characterize results via metrology methods described in the following sections of this paper. Since it is well known that welding can grossly distort even the heaviest of structural members, the goal is to minimize beam distortion, establish cold stress relieving methods, and quantify the net distortion due to the weld process with the goal of minimizing this effect. Since it will be impossible to prevent all distortion of the ideal shape desired, the bearing system of the tracker has been designed to accommodate reasonable departures from the ideal geometry.

3. MEASUREMENT SCOPE & REQUIREMENTS

System Mount Model

The tracker test stand, tracker drive axes, and sub assemblies such as the PFIP (including WFC), and bridge, will be set up and verified to the accuracy limits of a laser tracker (about 1 part in 200,000). The entire mechanical system is designed to perform so that deviations from the ideal motions of each axis are: 1) within a known and acceptable range, 2) immune to vibration (modal behavior), 3) are definable by some independent metrology method, and 4) are repeatable. It is assumed that if the engineers, designers, and fabricators have correctly done their job that 1, 2 and 4 are sufficiently under control and that 3 will ultimately be sensed by the most critical of all detectors: the telescope itself, unless these deviations are compensated for by the drive axes and control algorithms of the Telescope Control System. With a mechanical system as complex as the HET it is very difficult and time consuming to de-convolve an errant axis that is responsible for a drifting image on the detector, so we are motivated to characterize (measure) and write compensating control algorithms for each drive axis independently, to a level of precision that supports the ultimate system positioning accuracy specification. In the case of the HET, we identify the position within the entire optical system that needs to track a star image as the Stationary Image Rotation Point (SIRP)[14-19] on the WFC. This point is so named because tips and tilts about this position do not result in a corresponding scan motion on the sky. Optical tolerancing analysis has established a cylindrical envelope located at the SIRP within which a star image must be maintained in order to meet the image quality specification for the telescope system. This cylindrical envelope, aligned with the WFC optical axis, is +/- 10 μm long x 10 μm radius and must maintain an angular relation to the optical (W) axis (see Figure 2) to within +/- 4 arc-seconds. Table 1 shows the relative measurement accuracy, or in some cases absolute accuracy desired to characterize each axis in order to create a compensation table for each axis in the laboratory, or on the telescope.

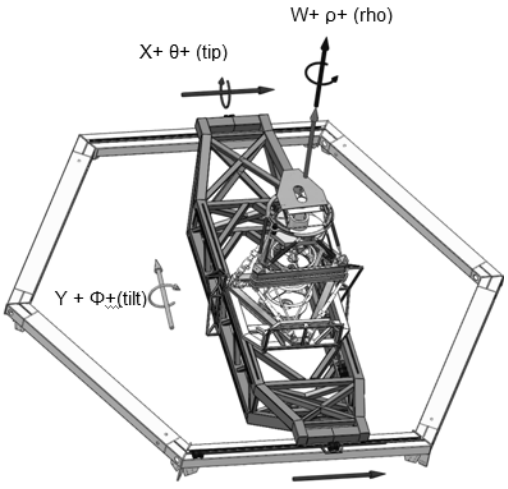

Figure 2: Tracker coordinate system axes.

It is clear, by inspection that the upper and lower X-axes will have their own unique characteristics, due to the fact that the lower axis supports substantially greater load and is reinforced uniquely. In addition, however, there are asymmetric features to the right and left beam trusses of the tracker bridge, with a primary and secondary side respectively, that require measurement of each in order to build the

complete mount model. Also, due to the design of the hexapod supports, the front lower joint of the hexapod, or the leading corner of the Lower Hexapod Frame (LHF) must be separately characterized since its deflection will be a function of hexapod tilt about the SIRP (or Y-position). Thus, although there are 10 drive-axes of motion on the tracker, in reality there are 3 more which derive from various features of the mechanical design, and as will become clear in the discussion of the "on-telescope" mount model, a number of additional degrees of freedom that derive from structure and foot-pad deformations due to the shifting mass of the tracker on the upper hexagon.

Axis	X(μm)	Y(μm)	Z(μm)	W(μm)	ρ(arcsec)	Θ(arcsec)	Φ(arcsec)
Upper-X	+/-10	+/-10	+/-10	-	-	-	-
Lower-X	+/-10	+/-10	+/-10	-	-	-	-
Y-primary	+/-10	+/-10	+/-10	-	-	-	-
Y-secondary	-	-	+/-10	-	-	-	-
LHF+	-	-	+/-34	-	-	-	-
Hexapod System*	+/-10	+/-10	-	+/-10	+/-3	+/-4	+/-4
Rho	+/-10	+/-10	-	+/-10	+/-3	+/-4	+/-4

+ Front corner of the LHF.

* Corners of Upper Hexapod Frame (UHF) relative to corners of the LHF.

Table 1: Measurement accuracy desired for each axis relative to the telescope coordinate system.

Tracking Performance

The purpose of the tracker is to align the optical axis (W-axis) of the WFC normal to the spherical primary mirror, and to position the SIRP of the WFC on the spherical focal surface of the primary mirror, and to change that position as a function of time in order to track celestial objects. As stated previously, the tolerance for this position at any time is defined by the +/-10μm long x 10μm radius x +/-4 arc-sec cylindrical envelope. The goal of performance verification measurements in the lab is to: 1) determine the time-resolved position of the SIRP along any predetermined path on the tracking sphere, 2) resolve the extent and frequency of "jitter" of the SIRP, 3) determine the effect of simulated "guide corrections", and 4) evaluate the initial positional accuracy and trajectory of the SIRP at the beginning of a track following "rewind", or slew, to a new tracking position. Since the SIRP is an optical datum, its position is inferred by referencing to the outer corners of the Mirror 2 (M2) support truss at the bottom of the WFC. Table 2 displays the accuracy goal for measurements of any one of these corner positions in order to resolve the SIRP position while tracking.

Datum	X(μm)	Y(μm)	Z(μm)	ρ(arcsec)	Θ(arcsec)	Φ(arcsec)
SIRP (virtual)	+/- 3.3	+/- 3.3	+/-3.3	+/- 4	+/- 4	+/- 4
WFC Bottom Corner	+/- 3.3	+/- 3.3	+/- 3.3	+/- 4	+/- 4	+/- 4

Table 2: Measurement accuracy goal for SIRP and reference points relative to the telescope coordinate system.

4. MEASUREMENT TECHNIQUES INVESTIGATED

Laser Tracker

Laser trackers can generally be configured to produce precision measurements of a 3D coordinate to 1 part in 200,000 (2 σ). In interferometric mode (along the optical axis of the laser), they can resolve a target to 1 part in 666,000 relative to another in the same data set as long as the optical path is unbroken between measurements and originates from a reference position on the laser tracker. Measurements made orthogonal to the beam are resolved by rotary encoders and typically have accuracy ratings that diverge on the order of 3.5μm/m, with reports of improved resolution in recent models. Using a laser tracker in interferometric mode is difficult over a 10 meter x 10 meter x 5 meter assembly which is tilted at 35°, like the new tracker, since a single target must be physically moved and positioned at various points of interest without losing line-of-sight to the laser. An alternate, but less precise mode is to position targets at multiple points of interest on the assembly and program the laser tracker to visit and measure each target in succession. In this mode, time-of-flight calculations are made (know as Automatic Distance Measuring or ADM) which requires simultaneous input of temperature and atmospheric pressure to assure proper calibration, and are generally good to the 1 part in 200,000 figure. The cost for each target is on the order of US$2k, making cost an important consideration for automated multipoint measurements. Generally speaking lasers are most accurate when they can dwell long enough on a static point to record thousands of measurements per second and establish a mean and standard deviation for the result, but they can also perform time or distance resolved measurements to nearly equivalent accuracy. As-built measurements were performed on the HET using an API Tracker3, and over a distance of 22 meters, time-resolved measurements, where the HET tracker position was measured while in slew mode (80 mm/sec) and were found to be good to 1 one part in 188,000 (1.65 σ). Testing of laser trackers in the laboratory have demonstrated the importance of having a quiet and stable mount. Vibration in the laboratory floor is a key concern in the use of this technique.

Photogrammetry

State of the art photogrammetry (PG) methods can produce simultaneous measurements of 3D coordinates to 1 part in 150,000, limited only by the number of targets you wish to set up in the target volume. Even though PG offers lower accuracy in comparison to laser trackers, the technology was thoroughly investigated because it was seen to be a labor saving way to enable measurement of numerous targets in one interval over the target volume of the tracker (10 meter x 10 meter x 5 meter tilted at 35°), as well as the volumes of smaller assemblies like the PFIP and WFC. In addition, the measurement results are comparatively noise-free since the technique is only sensitive to vibration in the target, and not simultaneously in the measurement device, as is the case for laser trackers, which are often mounted to the same floor that may be driving vibrations in the target. However, the cost of proprietary high-performance PG systems is at parity with that of laser trackers, and PG systems are not particularly suited to perform high-accuracy time-resolved measurements without considerable additional investment in cameras, strobes, and data handling capability, due to the need for 4 or more cameras, required to capture simultaneous images to resolve moving targets. Excellent PG introductory tutorials are available from online and published sources, which cover the fundamental theory of this technique. A few of the less obvious lessons-learned are noted here.

The essential elements of a high-accuracy target-based PG system are comprised of; a stabilized camera, bundle adjustment software, reflective targets, and scale bars. In the case of the camera, the accuracy achievable is a function of pixel density, and body and lens stability. Advances in the stability of camera bodies, and large CCD's (for instance the Nikon D3X, with 6048 x 4032 CCD) make it possible to buy this component off-the-shelf instead of through a PG manufacturer. The D3X is built on a metal chassis which contributes to the stability over the life-time of the system. Cameras with plastic frames have a life-time of about 100k exposures before stability problems arise, due to loss of mechanical tolerances from wear. On a similar theme, the lens can also be purchased off-the-shelf as a cost saving measure. The lens is typically selected to provide a 90° field of view and, if possible, fill the entire area of the detector. The lens is stabilized by soft clamping, or completely locking movement of the mobile components in the optical assembly, like focusing (requiring dis-assembly and re-assembly of the lens: usually in the skill set of this audience). The mounting interface between the camera body and lens is considered to be essentially stable, but not necessarily repeatable if removed and then replaced (requires re-calibration of camera). Thermal stability of the camera is sufficient if it is very close to the temperature at calibration. If the camera is being hand-held, which is almost always the case, it should be handled in 5 minute intervals, or less, or be thermally isolated from body heat. Since there is typically a need for good focus on the targets throughout the subject being measured, it is necessary to have the f-stop set at, or near minimum (small iris). Since this reduces the image signal, reflective targets are used in conjunction with a ring-type

electronic strobe mounted on the lens to provide source lighting and exposure control. This produces very clear, high signal-to-noise images of the targets in the image. Care must be taken to not over expose the target since this can saturate the CCD and cause significant error in the calculation of the target location by the software. Often the object being measured is substantially under-exposed in the images, but it can be enhanced with image processing tools contained in the bundle adjustment software, in order to identify its features. The size of the smallest target (usually the most distant target) imaged on the CCD, is typically required to be on the order of 8 to 12 pixels in diameter. When combined with the distance from the target, and the camera characteristics, this establishes the required target size according to the formula:

$$\frac{(\text{target diameter on CCD in pixels}) \times (\text{most distant target}) \times (\text{width of CCD})}{(\text{total width of CCD in pixels}) \times (\text{focal length of lens})} = \text{target diameter}$$

Calibration of the camera is achieved by setting up a stable grid of reflective targets and taking 16 or more images for processing in the bundle adjustment software. If the image characteristics are strong enough in terms of all the usual criteria e.g. angles, camera rolls (rotations with respect to the horizon), image fill, number of photos (usually 25, or more), targets captured per photo, then further refinement of the initial camera calibration is typically performed by the software during processing of the actual data set. The normal camera settings must be turned off since these can compromise the stability of the CCD or the image exposure. For instance, the Nikon D3X uses piezo-electric actuators, which are useful in conventional photography to sharpen focus at the corners of the image, or induce vibrations (using the same piezos) to remove dust from the detector surface. Once the exposure settings are established by taking test images, the f-stop and shutter speed are held constant to assure uniform exposure of the targets throughout the image set. In addition, color mode is suppressed, since the image analysis routines are typically optimized for gray-scale. JPEG image compression is allowed, and is in fact advantageous, since it reduces the file size and speeds up processing of the images.

Bundle adjustment software is proprietary and the heart of the PG system. It involves years of development and refinement by highly skilled programmers who are also specialists in image processing mathematics. Most software systems are designed to work as a package system with included cameras, coded targets, and scale bars. Specifically, the software will typically only work with that vendor's cameras and coded targets, thereby assuring: better control of results (through training and equipment quality control), accuracy, and allegiance to the brand purchased. At least one company has departed from this business model and allows the user to supply cameras and standardized coded targets. This company is Eos Systems, Inc. and the bundle adjustment software is called PhotoModeler®. They have numerous papers published by a great variety of customers, including NASA[?]. They also have well developed tutorials for self-teaching (which are free of charge), make training sessions available on a periodic basis, and are generally less proprietary in their disclosure of PG details. The software will accommodate images from multiple cameras which can be useful in cases where time-resolved measurements are desired. Their product is also lower in cost by a substantial margin. In the processing of images, targets are typically located using one of two processes. The faster, but less accurate method calculates the Centroid of the target image and, uses this as the location. The more accurate method of target image location is Least Squares Matching (LSM).

Reflective targets are a subtle and important feature of the PG technique, assuming one wants to push accuracy near the theoretical limits. As stated previously, it is necessary to correlate target size to the distance from the object, as well as the camera lens and detector. This tends to limit the flexibility of the technique, unless one is willing to stock a varied inventory of coded and un-coded targets. Sometimes the optimal target size is non-standard and needs to be custom made. The necessity for use of coded targets cannot be over emphasized, since this enables the software to automatically identify and correlate targets between images. Manual recognition of targets in most cases is prohibitively labor intensive. An additional consideration is precisely determining the offset of the reflective surface from the actual surface being measured. Typically reflective targets are composed of layers of reflective material covered by a mask. This mask can cast a dimensionally significant shadow across the reflective substrate, as well as contribute inaccuracy to the target offset from the reference surface. The thicknesses of the various layers needs to be uniform and well understood, which is inherently difficult to achieve with soft and flexible materials. Targets are also susceptible to damage and contamination and can lead to significant errors in the calculation of their location. The lack of target rigidity and flatness can also have an effect on accuracy.

The discussion of targets transitions well to that of scale bars, because it highlights one of the key issues to be aware of in using the PG method: that of achieving accuracy in measurements. Where laser trackers are dependent on well

understood laser wavelength for dimensional scaling, PG relies on calibrated scale bars, which are a generation removed from the absolute reference. In addition, scale bars are significant in cost and must have a meaningful length and target diameter (preferably coded), for the specific setup they are being used in. This, combined with the uncertainty in target placement, limits PG usefulness in determining absolute distances between features of the object being measured. The strength of PG is in detecting movement of targets, once their position has been established, such as thermal, or load deformations on an object.

In the end, laser tracker technology is favored by this project, over PG, because of its accuracy, versatility, ease of learning and use, and budget constraints limiting our investment to one metrology system.

Data reduction

Streamlining the processing and fitting of data is as important as taking accurate measurements. PG software typically offers some basic data fitting capability, but an important consideration in building a metrology system is the purchase of a data processing/fitting software package. At least three products are written which receive data from practically every kind of digital measurement device (including laser trackers and PG), and depending on options purchased, will directly correlate measurements to CAD models of objects being measured. These three products are: Spatial Analyzer®, VeriSurfX®, and PolyWorks®. This project chose VeriSurfX®, based upon academic pricing, and familiarity with MasterCam® software that operates in the background of this application.

5. LABORATORY MEASUREMENTS DESIGN

The goal of the laboratory measurements is to, as directly, accurately, and cost-effectively as possible, quantify the systematic errors in the motions of the tracker payload and to use this information to create the tracker mount model for incorporation into the tracker controls.

X & Y Axis Characterization

Figure 2 illustrates the concept for using a single laser tracker underneath the test stand for measurement of the tracker as it is translated by the X and Y axes. Reference Sphere Mounted Reflector (SMR) targets are mounted at the 4 corners of the test stand, and an additional SMR is mounted on a corner of the tracker bridge, or on the carriage of the Y-axis. The position of the target is measured as the tracker slews, tracks, or dwells in a particular location. The Y-axis payload is varied in location in order to characterize the upper and lower X-axes as a function of shifting payload in the Y-axis. In a similar manner, the primary and secondary trusses of the bridge are characterized due to shifting center of mass (CoM) of the PFIP assembly as a function of X-axis and Y-axis position. As mentioned in section 3, it will be necessary to also characterize the deflections of the front joint of the lower hexapod frame as a function of Y-axis PFIP CoM. This set of measurements will provide the foundational mount model for the 7 axes above the Y-axis carriage. The worst case accuracy of measurements in this proposed set-up is predicted to be +/-33 μm (1.65 σ), or better.

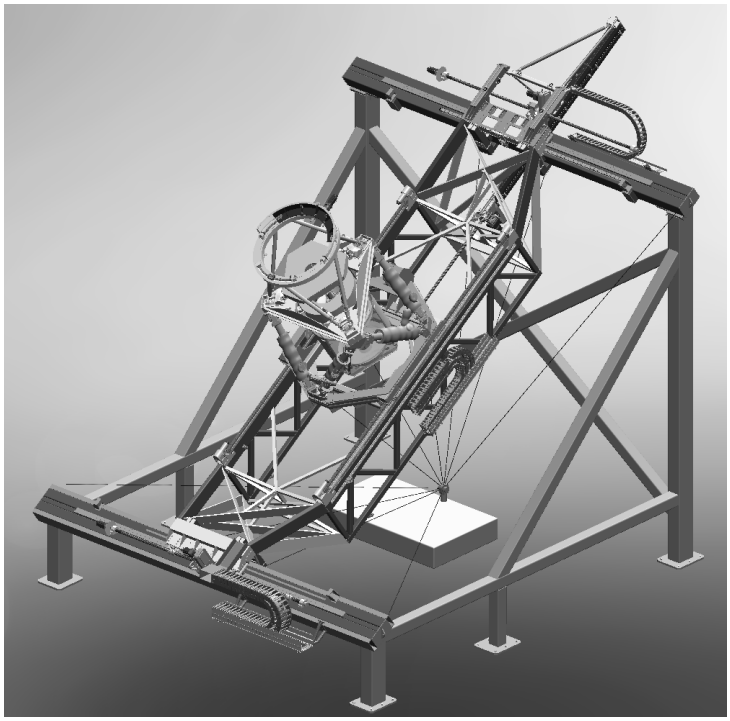

Figure 3. A laser tracker, set up on a stable platform, is positioned to access 4 corner references as well as multiple points of interest on the tracker.

Initial Hexapod Characterization

An initial hexapod mount model will be determined in two steps prior to assembly on the tracker. The first step will characterize the behavior of the individual actuators of the 6-strut assembly on a test stand designed specifically for

this purpose. The measurement, performed by a Heidenhain linear encoder, has an accuracy of +/- 2 μm. The test stand, with a prototype hexapod actuator mounted in it is shown in Figure 4. Following determination of systematic errors in the individual actuators, the hexapod assembly will be assembled on a hexapod test stand, and measured using a laser tracker, as shown in Figure 5. As proposed, the laser tracker can be programmed to scan and measure 6 targets in under a minute and remove the effect of most deflections in the test stand by monitoring the position of the hexapod base to within +/-9 μm. The upper hexapod frame (a.k.a. strongback) for mounting the WFC and upper PFIP assembly, can be monitored to within +/-14 μm.

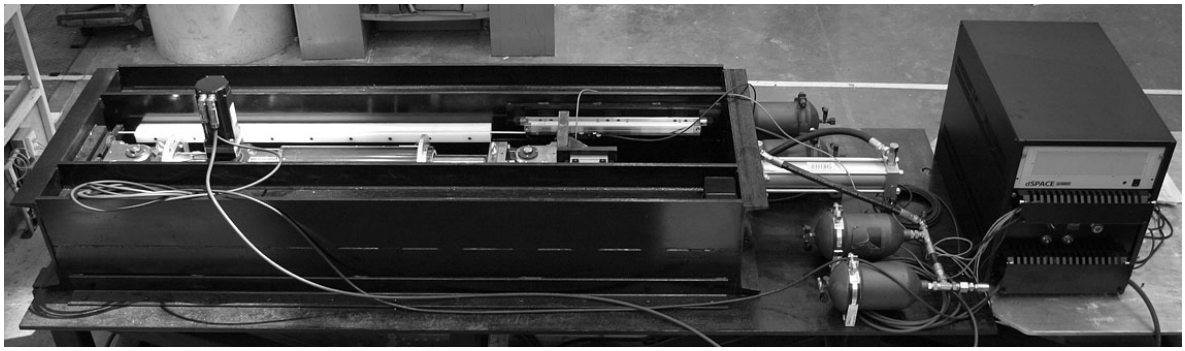

Figure 4. Prototype actuator for the hexapod shown mounted on the test bench at CEM.

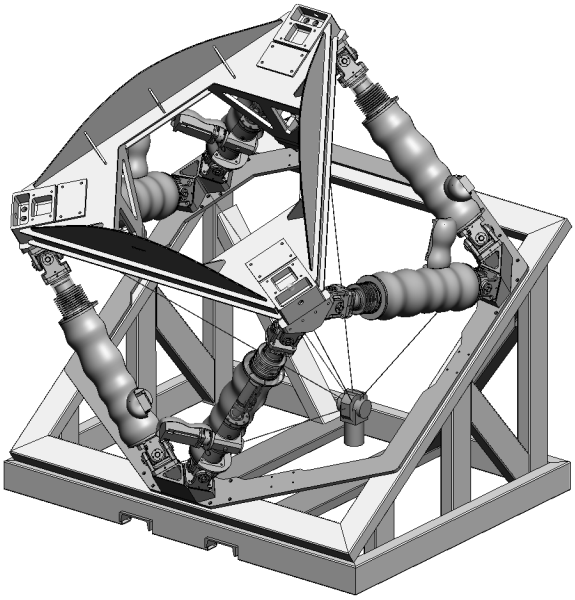

Figure 5. The hexapod in testing configuration on its test stand with laser targets positioned at the corner nodes.

PFIP Alignment and Characterization

The Prime Focus Instrument Package (PFIP) is comprised of the WFC and a passive hexapod structure which serves to support the WFC in relationship to optical fibers at its focal surface. It also supports the Rho stage (interposed between the passive hexapod and the focal surface) as well as instrumentation in support of guiding, exposure control, wave-front sensing, atmospheric dispersion compensation, and support interfaces for current instrumentation on the HET such as the High Resolution Spectrometer (HRS).

For the purposes of alignment and measurement of deflections, the PFIP will be mounted on the hexapod while it is in the test stand (as discussed for the hexapod measurements). WFC alignment to the focal surface is accomplished in three major steps. The first is to 'level' the WFC with respect to its mounting structure, otherwise known as the 'strongback', (a.k.a. the upper hexapod frame). The strongback contains 3 V-grooves oriented to converge at the optical axis in the center of the PFIP. The WFC support structure contains a set of 3 spheres which mate with these grooves in

order to establish a highly repeatable kinematic mount. The mechanical design of the spheres includes allowance for shims to adjust their relative height. The shim thickness will be determined by test fitting the WFC to the strongback and measurement by means of a laser tracker. The precision of this measurement (+/-15 μm, or better) will likely allow the fitting of these shims in a single iteration, followed by a repeat of the assembly and measurement for verification. The second step (Figure 6) is accomplished by use of the laser tracker to tune-in and lock the adjustable struts of the passive hexapod while it is oriented 35° with respect to gravity. This procedure will rough-in the focal surface and will involve measuring the curved path of the Rho axis bearings and comparing their orientation in all 6 degrees of adjustment with respect to datums (established in step 1) located on the kinematic mount interface. The predicted accuracy of this step is +/-22 μm. A third procedure will utilize an alignment telescope and high-precision crosshairs mounted on specially designed center plugs for the M2 and M5 mirrors of the WFC. Both the alignment telescope and the crosshairs will have been aligned and fitted with highly repeatable kinematic mounts during the manufacture of the WFC. It should be noted that the WFC has a clear optical path going through the center of its four mirrors. This enables alignment telescope, mounted to the bottom of the WFC and aligned with the optical axis, to see fiducials along the optical axis. To establish a center reference for the Rho axis a flat ground plate with cross-hairs (mounted on an x-y translation stage) will be mounted on the Rho axis bearings and the cross hairs will be dialed-in by rotating and referencing to the central datum of the alignment telescope. The Rho-axis cross-hairs will then be compared to those of the center plugs through the alignment telescope. Final adjustment of the passive hexapod legs will be performed to align the series of 3 cross hairs, and iterative checks of planarity and focus will be checked by laser tracker and adjusted as described in step 2. The predicted accuracy of this alignment is +/- 5 μm.

At this point the PFIP can be measured its deflections. It should be restated that while tracking, the PFIP will be tilted by the hexapod +/-8.5° with respect to its centered position, resulting in deflections in the support structure due to change in the gravity vector. The dimensional tolerance for displacements (due to these deflections) of the focal surface with respect to the WFC optical axis (X,Y) and focus (W) is shown in Table 3. These deflections can be quantified by tilting the PFIP to the +/-8.5° position (as well as intermediate angles) and re-centering the Rho-stage crosshairs on the WFC crosshairs and alignment telescope. The adjustment in the x-y stage required to re-superimpose the crosshairs will correspond to the deflection and is measured by a common linear digital gauge to +/-1 μm precision.

Item	Tip/tilt [degrees]	Decenter [μm]	Defocus [μm]
Tolerance	± 0.1	± 31.7	-111.8 / +62.6

Table 3. Final misalignment tolerance (peak-to-peak) of the FPA set by the top-level requirements

WFC & SIRP Tracking Measurements

The mount model created by measurement and determination of the systematic errors of the X, Y, hexapod drive axes, PFIP structure, as well as special case deflections of the primary and secondary bridge trusses and lower hexapod frame will be ultimately tested in the laboratory by watching the SIRP as it follows a tracking trajectory. This tracking trajectory will be a path generated in the Telescope Control System (TCS) which is on the theoretical tracking sphere. The tracker's ability to follow this path will be monitored in the laboratory by up to three laser trackers placed in closest possible proximity to the bottom of the WFC. Three laser targets (SMRs) will be placed on the bottom corners of the support structure of the WFC, which will have a known dimensional relationship to the SIRP. To meet budget requirements, initial tests will use only one laser tracker, which will rove from target to target in order to provide very good measurements of tracking behavior. Since the repeatability of the system can be tested to high precision and will likely be proven to be quite high, it is possible that repeating the identical computer-generated tracking trajectory three times, using one laser tracker to measure a different corner each time, will provide sufficient information to prove required performance. Ultimately, however, since laser trackers cannot sense rotations, measurements are being proposed that use three laser trackers, in order to prove that the system is following the commanded trajectory. The accuracy predicted over a 2 meter track is +/-2.5μm (1.65 σ). A single laser, or trio of lasers, can be positioned to follow a full 4 meter trajectory, which a predicted accuracy of +/24μm (1.65 σ).

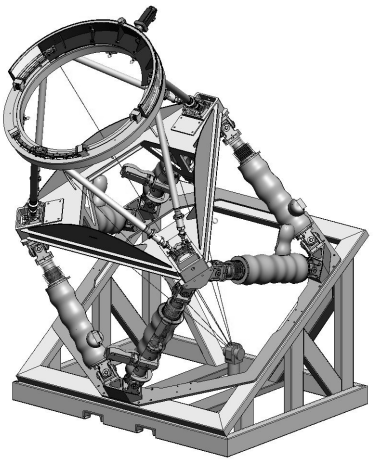

Figure 6. The Prime Focus Instrument Package structure mounted on the hexapod in testing configuration with laser targets positioned at the corner nodes.

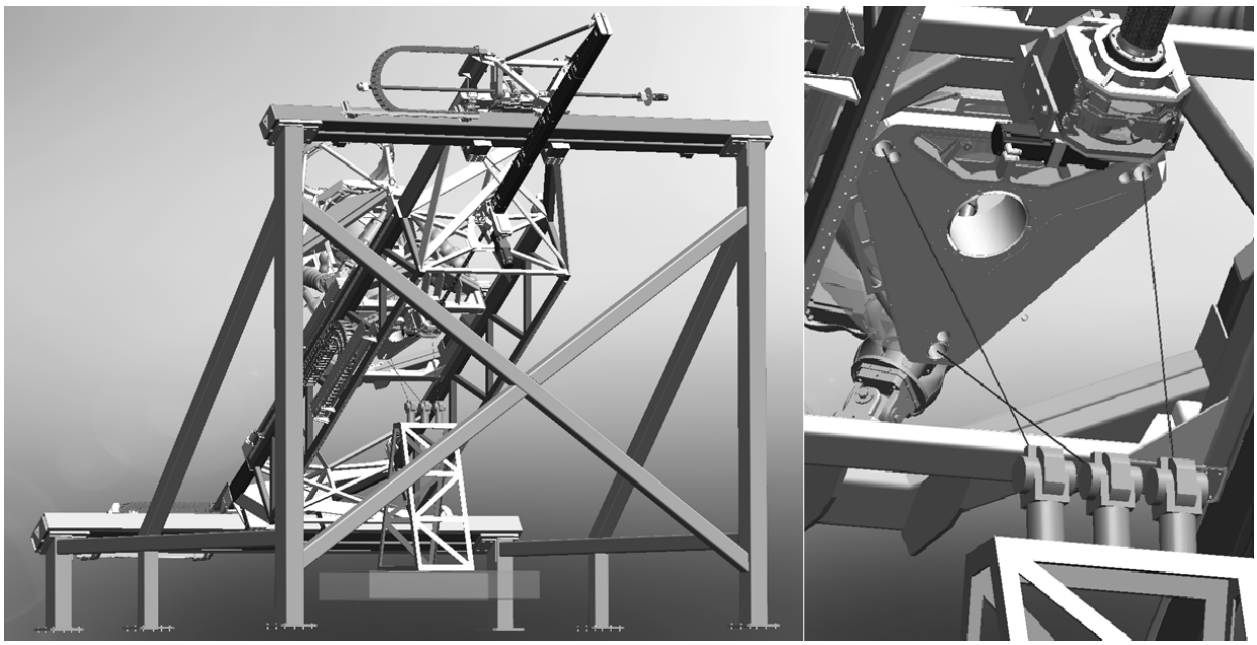

Figure 7. Proposed configuration for sensing the fidelity of motion on the tracking sphere using up to three laser trackers for sensing the position of the three lower corners of the WFC.

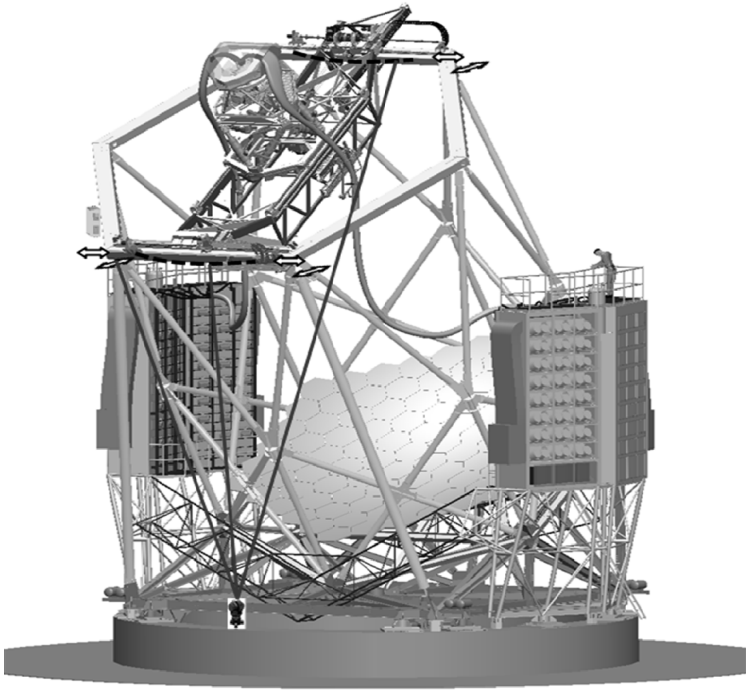

Figure 8. Proposed laser tracker positioning for measurements of upper and lower X-rail deflections, as well as tip and tilt of the HET structure during tracking.

6. ON-TELESCOPE MEASURMENTS

When the new tracker is removed from the test stand in Austin and placed on the telescope in West Texas several additional elements of the mount model will have to be defined. Even though the telescope structure sits stationary on 4 foot pads during observations, the 5x increase in mass is predicted to produce significantly more pronounced tip and tilt deflections about the base of the structure as the payload CoM shifts on the upper hexagon during tracking. Additionally, the upper and lower X-rails of the tracker will have different profiles and deflections from those measured and modeled into the TCS in the laboratory. Figure 8 illustrates using the laser tracker to measure these deflections to 1st order. In the configuration shown, with the laser mounted on the azimuth pier, the lower rail, as well as tip and tilt motions of the entire upper hexagon, should be quantifiable to within +/-70 μm of the actual deflections. The upper rail can be determined to within +/-100μm. Substantially higher accuracy (+/- 30 μm) can be achieved if required by using three laser trackers in interferometric mode, to triangulate targets on

the upper hexagon. Additionally, since we will be in a position at this point to go on sky, it will be possible to use the laser in tandem with observed guiding errors, to monitor the effect of adjustments to the mount model for these particular deflections in the mechanical system

7. SUMMARY

The measurement methods proposed should be sufficient for determining and testing corrections to systematic errors in the individual tracker axes of motion and creating an initial mount model for the new Wide Field Corrector. Since these are only tests of the mechanical performance and not the optical performance of the system, modification to the tracking model will be required once it is installed on the telescope. However, the techniques proposed should provide a high degree of confidence in the performance of the mechanical system and its controls prior to retro-fit on the HET and reduce time for commissioning on the telescope.

REFERENCES

[1] Hill, G.J., Gebhardt, K., Komatsu, E., Drory, N., MacQueen, P.J., Adams, J.A., Blanc, G.A., Koehler, R., Rafal, Roth, M.M., Kelz, A., Grupp, F., Murphy, J., Palunas, P., Gronwall, C., Ciardullo, R., Bender, R., Hopp, U., and Schneider, D.P., 2008, "The Hobby-Eberly Telescope Dark Energy Experiment (HETDEX): Description and Early Pilot Survey Results", in Panoramic Views of the Universe, ASP Conf. Series, vol **399**, p 115 (arXiv:0806.0183v1)

[2] R.D. Savage, et al., "Current status of the Hobby-Eberly Telescope wide field upgrade and VIRUS," Proc. SPIE, **7012**-10 (2008)

[3] G.J. Hill, et al., "VIRUS: a massively replicated 33k fiber integral field spectrograph for the upgraded Hobby-Eberly Telescope," Proc. SPIE, **7735**-21 (2010)

[4] H. Lee, et al., "LRS2: a new low-resolution spectrograph for the Hobby-Eberly Telescope and its application to scalable spectrographs for the future of extremely large telescopes," Proc. SPIE, **7735**-276 (2010)

[5] J.T. Heisler, et al., "Integration of VIRUS spectrographs for the HET dark energy experiment," Proc. SPIE, **7733**-153 (2010)

[6] J.A. Booth, et al., "Wide Field Upgrade for the Hobby Eberly Telescope," Proc. SPIE, **6267**, 2006

[7] J.H. Burge, et al., "Development of a wide-field spherical abberation corrector for the Hobby-Eberly Telescope," Proc. SPIE, **7733**-51 (2010)

[8] M.S. Worthington, et al., "Design and analysis of the Hobby-Eberly Telescope dark energy experiment (HETDEX) bridge," Proc. SPIE, **7733**-147 (2010)

[9] N.T. Mollison, et al., "Design and development of a long-travel positioning actuator and tandem constant force actuator safety system for the Hobby-Eberly Telescope wide field upgrade," Proc. SPIE, **7733**-150 (2010)

[10] G.A. Wedeking, et al., "Kinematic optimization of upgrade to the Hobby-Eberly Telescope through novel use of commercially available three-dimensional CAD package," Proc. SPIE, **7733**-148 (2010)

[11] J.J. Zierer, et al., "The development of high-precision hexapod actuators for the Hobby-Eberly Telescope dark energy experiment (HETDEX)," Proc. SPIE, **7733**-49 (2010)

[12] J.R. Mock, et al., "Tracker controls development and control architecture for the Hobby-Eberly Telescope dark energy experiment," Proc. SPIE, **7733**-152 (2010)

[13] B.J. South, et al., "Wind loading analysis and strategy for deflection reduction on the HET Dark Energy Experiment upgrade," Proc. SPIE, **7733**-51 (2010)

[14] M.S. Worthington, et al., "Design and development of a high-precision, high-payload telescope dual-drive system," Proc. SPIE, **7733**-201 (2010)

[15] H. Lee, et al., "VIRUS optical tolerance and production," Proc. SPIE, **7735**-140 (2010)

[16] H. Lee, et al., "Analysis of active alignment control of the Hobby-Eberly Telescope wide field corrector using Shack-Hartmann wavefront sensors," Proc. SPIE, **7738**-18 (2010)

[17] H. Lee, et al., "Surface figure measurement of the Hobby-Eberly Telescope primary mirror segments via phase retrieval and its implications for the wavefront sensing in the new wide-field upgrade," Proc. SPIE, **7738**-58 (2010)

[18] H. Lee, et al., "Orthonormal aberration polynominals over arbitrarily obscured pupil geometries for wavefront sensing in the Hobby-Eberly Telescope," Proc. SPIE, **7738**-59 (2010)

[19] H. Lee, et al., "Metrology systems for the active alignment control of the Hobby-Eberly Telescope wide-field upgrade," Proc. SPIE, **7739**-28 (2010)